Simulation of the Femtosecond Optical Response of a Solute in Water

Laurence E. Fried, Nathan Bernstein, and Shaul Mukamel
Department of Chemistry, University of Rochester, Rochester, New York 14627
(Received 9 August 1991)

We present microscopic semiclassical simulations of the femtosecond nonlinear optical polarization ($P^{(3)}$) of a solute in water. $P^{(3)}$ is dominated at short times by intermolecular vibrations that cannot be accounted for by the Bloch equations. The applicability of the Bloch, stochastic, and Brownian oscillator models to the interpretation of photon echo and pump-probe measurements is discussed. We find that only microscopic semiclassical simulation and the Brownian oscillator model can account for the essential features of $P^{(3)}$.

PACS numbers: 42.65.−k, 78.20.−e

Femtosecond nonlinear optical spectroscopy of dyes in liquids cannot be interpreted using the Bloch equations. The system has a multitude of relaxation time scales and in general they cannot be considered to be either infinitely fast (homogeneous broadening) or infinitely slow (inhomogeneous broadening) on the experimental time scale. This state of affairs was recently highlighted by photon echo (PE) measurements in polar liquids [1,2]. The nonexponential decay of the PE found in these experiments indicates that the Bloch level of description is inadequate. The origin of the non-Bloch behavior in liquids is the continuous distribution of solvent time scales, rather than the strong field effects related to the Rabi frequency observed previously [3].

In this Letter we present a microscopic semiclassical simulation [4,5] of the nonlinear polarization $P^{(3)}$ of a dye in water. We reproduce many essential features of the recent experiments, including the non-Bloch behavior of the photon echo signal. We use the results of our simulation to test the Brownian oscillator model [6], the stochastic model [7,8], and the Bloch equations. This allows us to determine the level of theoretical modeling sufficient to interpret these recent experiments. Previously, photon echo signals in polar liquids have been interpreted using the stochastic model in the limit of an overdamped solvent [1,2]. Our simulations show that intermolecular vibrations are very important in the short-time optical polarization of a solute in a polar liquid. We find that only the Brownian oscillator model and microscopic simulation can reproduce the essential features of the nonlinear optical polarization of a solute in a polar liquid.

The present microscopic semiclassical approach is derived by taking the classical limit of exact quantum expressions for $P^{(3)}$ [4,5]. It takes into account a distribution of solvent time scales and the difference between dynamics in the ground and excited states of the chromophore. The Brownian oscillator model is a limiting case of the microscopic semiclassical theory applicable when the ground- and excited-state dynamics are similar. The stochastic model, in turn, can be derived from the Brownian oscillator model by assuming an overdamped solvent and neglecting the effect of the solute on the solvent. This means that solvation dynamics is completely missed. Finally, the Bloch equations may be derived from the stochastic model by assuming that the solvent has only infinitely fast and infinitely slow time scales. The four methods thus constitute a hierarchy of approximations.

In our simulation the solute is assumed to have two relevant electronic states, $|g\rangle$ (the ground state) and $|e\rangle$ (the excited state). The Hamiltonian for this system in the presence of an electric field $E(t)$ is $H_T = H - VE(t)$, where

$$H = |g\rangle H_g(Q)\langle g| + |e\rangle H_e(Q) + \omega_{eg}\langle e|$$

and $V = |e\rangle\mu\langle g| + |g\rangle\mu\langle e|$. Here H_g and H_e are the adiabatic Hamiltonians of the solute plus solvent system. The set of all nuclear positions is represented by the vector Q. ω_{eg} is gas phase 0-0 absorption frequency of the solute. Below, we neglect the dependence of the dipole operator on nuclear position (Condon approximation), the internal vibrations of the solute, and the solute motion during optical probing.

H_g and H_e are of the form $H_i = T + V^{(\mathrm{W\text{-}W})} + V_i^{(\mathrm{W\text{-}S})}$, where $i = g,e$, T is the kinetic energy, $V^{(\mathrm{W\text{-}W})}$ is the water-water interaction (taken to be the same in the ground and excited electronic state), and $V_i^{(\mathrm{W\text{-}S})}$ is the water-solute interaction. Both the water molecules and the solute were taken to be rigid. Interaction site models were used for the potential between molecules; i.e., the jth atom of each molecule was assigned Lennard-Jones parameters σ_j, ϵ_j and a partial charge q_j. This leads to the atom-atom potential form

$$V^{(\mathrm{atom\text{-}atom})}(r_{ij}) = \frac{q_i q_j}{r_{ij}} + 4(\epsilon_i\epsilon_j)^{1/2}\left[\left(\frac{\sigma_i+\sigma_j}{2r_{ij}}\right)^{12} - \left(\frac{\sigma_i+\sigma_j}{2r_{ij}}\right)^{6}\right], \quad (1)$$

where r_{ij} is the distance between atoms i and j. The simple point charge–enhanced potential [9] provided parameters appropriate to water. The solute had one Lennard-Jones site ($q_j = 0$) at the molecular center of mass with $\epsilon = 70\ \mathrm{cm}^{-1}$ and $\sigma = 4$ Å. The Lennard-Jones site was

taken to be the same in the g and e states. In addition, the solute in the excited state had two fixed charge sites ($\epsilon_j = 0$) with opposite charges of magnitude $q_j = e$ located at positions (0,0, ± 0.25 Å). This model represents a typical nonpolar dye molecule with a large dipole moment in the excited electronic state.

The signal $S_{3PE}(t_1,t_2)$ in the three-pulse photon echo (3PE) is given by $S_{3PE}(t_1,t_2) = \int_0^\infty dt_3 |P^{(3)}(t_3,t_2,t_1)|^2$, where t_1 is the delay between the first two pulses, t_2 is the delay between the second and third pulses, and t_3 is the interval between the third pulse and detection. The ordinary photon echo is a special case of the 3PE: $S_{PE}(t_1) = S_{3PE}(t_1,t_2=0)$. $P^{(3)}$ can be expressed as a sum of two terms [6]: $P^{(3)}(t_3,t_2,t_1) = P_e^{(3)}(t_3,t_2,t_1) + P_g^{(3)}(t_3,t_2,t_1)$.

$P^{(3)}$ has the following interpretation: The first pulse sets up an optical coherence in the sample. During t_1 the evolution (and dephasing) of this coherence occurs. The second pulse converts the optical coherence into a population on either the ground ($P_g^{(3)}$) or excited ($P_e^{(3)}$) electronic state. During t_2 thermal fluctuations occur and the system relaxes toward equilibrium. This relaxation leads to the Stokes shift in $P_e^{(3)}$. The third pulse converts the population back into a coherence, which dephases during the t_3 evolution.

The microscopic semiclassical approximation for $P^{(3)}$ [4,5] (for pulses that are short compared to pure dephasing and molecular time scales) is

$$P_e^{(3)}(t_3,t_2,t_1) = \int dQ\,dP \exp\left[i\int_{t_2}^{t_2+t_3} U(Q[t',t_1])dt'\right]\exp\left[-i\int_0^{t_1} U(Q[t'])dt'\right]\rho_g(Q,P),$$
$$P_g^{(3)}(t_3,t_2,t_1) = \int dQ\,dP \exp\left[i\int_{t_2}^{t_2+t_3} U(Q[t'])dt'\right]\exp\left[-i\int_0^{t_1} U(Q[t'])dt'\right]\rho_g(Q,P). \quad (2)$$

Here $U \equiv V_g^{(W\text{-}S)} - V_e^{(W\text{-}S)}$. ρ_g is the classical Boltzmann distribution of the g potential surface. $Q[t]$ is defined as the coordinate of initial condition (Q,P) propagated for a period t with classical mechanics on the ground-state (g) surface. $Q[t_2,t_1]$ is defined as the coordinate of (Q,P) propagated for a time t_1 on the g surface, and then time t_2 on the e surface.

We evaluated Eq. (2) by performing a constant-energy molecular-dynamics simulation with 100 water molecules and 1 solute. Periodic boundary conditions were used, with the box size adjusted to give a density of 1 g/cm^3. The reaction field method [10] was used to correct for the presence of the long-range Coulomb forces. Because of the ergodicity of the fluid, we were able to generate initial conditions (Q,P) by taking samples at intervals along a single trajectory on the ground potential surface. This "base" trajectory was generated by starting from a random initial condition and then performing a Monte Carlo equilibration for 30000 cycles. The equilibrated configuration was used for the initial coordinate of the base trajectory. Initial velocities for the base trajectory were chosen from the Boltzmann distribution. The base trajectory was run for a time of 120 ps using a time step of 0.9 fs. The coordinate along the base trajectory gave $Q[t]$. Every 256th step, a secondary trajectory was run on the excited-state surface for 1024 steps. This served to generate $Q[t_2,t_1]$. The total length of the simulation, including both base and secondary trajectories, was 600 ps.

We first consider the ground-state and excited-state dynamics generated by the simulation. The autocorrelation function of $U(Q[t])$, $C(t) \equiv \langle U(Q[t])U(Q[0])\rangle - \langle U(Q[0])^2\rangle$ (where $\langle\rangle$ denotes thermal expectation value), is directly relevant to spectroscopic measurements. Within the Brownian oscillator model all spectroscopic observables are controlled by this autocorrelation function [6]. The mapping onto the Brownian oscillator model was achieved by attributing the classical simulation to the symmetrized correlation function $C(t) + C(-t)$, and using the fluctuation-dissipation theorem to get the complex $C(t)$ [6]. The stochastic model directly attributes the classical simulation to $C(t)$ which is therefore taken to be real [6]. $C(t)$ was evaluated along the base trajectory described above.

Figure 1 shows $C(t)$ for the solute in water. $C(t)$ is clearly in the intermediate modulation regime, where $\sqrt{C(0)}$ is of the same order of magnitude as the decay rate of $C(t)$. This is in accord with recent experimental

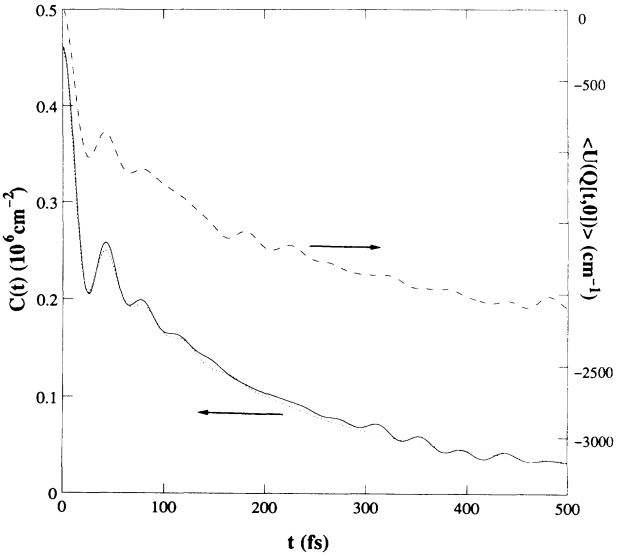

FIG. 1. Left scale: solid line, the autocorrelation of the energy gap $C(t)$; dotted line, fit by six Brownian oscillators. Right scale: $\langle U(Q[t,0])\rangle$.

results [1,2]. $C(t)$ shows a fast (period of 45 fs) vibrational component of the solvent relaxation [11]. The time-scale separation into very slow and very fast terms assumed by the Bloch equations is not apparent in the actual $C(t)$. In the Brownian oscillator model, $C(t)$ is the sum of N terms: $C(t)=C(0)\sum_i P_i C_i(t)$ [6]. Here P_i is the normalized weight of oscillator i. $C_i(t)$ depends on the oscillator's frequency ω_i and damping γ_i. Shown in Fig. 1 is a fit to $C(t)$ based on six Brownian oscillators. The parameters used (P_i,ω_i,γ_i) were (0.55,135,539), (0.18,817,277), (0.08,602,243), (0.07,452,439), (0.06, 379,420), and (0.04,49,752), where ω_i and γ_i are given in cm^{-1}. $C(0)=4.6\times10^5\ cm^{-2}$.

Figure 1 also shows $\langle U(Q[t,0])\rangle$ found upon excitation from the ground state to the excited state. Compared with the ground state, the excited-state dynamics shows a more prominent slow relaxation; while $C(t)$ has relaxed to within 5% of its asymptotic value with 500 fs, $\langle U(Q[t,0])\rangle$ has relaxed only to within 35% of its asymptotic value of $\approx 3400\ cm^{-1}$ within 500 fs. According to the Brownian oscillator model, $\langle U(Q[t,0])\rangle \propto C(t)$. The departure from this condition demonstrates that the Brownian oscillator model does not give a quantitative description of excited-state dynamics.

Linear and nonlinear spectroscopies provide a wide variety of "windows" onto the ground- and excited-state dynamics discussed above. PE, 3PE, and pump-probe spectroscopy probe different parts of $P^{(3)}$ and the underlying molecular dynamics. We begin our analysis with linear optics: The inset of Fig. 2 shows the ordinary absorption and fluorescence spectra, calculated by Eq. (2). The frequency ω is shown relative to ω_{eg}. Both spectra are broad and featureless, and hence contain little detailed dynamical information. The fluorescence displays a Stokes shift of about 3400 cm^{-1} to the red of the absorption line, while the Brownian oscillator model predicts a Stokes shift equal to 2200 cm^{-1}. The Stokes shift is missing in the Bloch equation and stochastic approaches.

In Fig. 2(a) we show the PE calculated with the $P_g^{(3)}$ term of Eq. (2) only [the quantum expression [6] for $P^{(3)}$ yields $P_g^{(3)}(t_3,t_2=0,t_1)=P_e^{(3)}(t_3,t_2=0,t_1)$]. The initial rise time is due to the finite inhomogeneous broadening in this system; in the limit of larger inhomogeneous broadening the induction time decreases. Nibbering, Wiersma, and Duppen [2] have observed a similar transient in the PE signal of sodium resorufin in dimethylsulfoxide. Also shown in Fig. 2(a) is the best fit of the Bloch equations to our simulated results. Clearly, the Bloch equations do not offer an adequate description of the initial transient.

Finally, Fig. 2(a) gives the results of mapping the present simulation onto the Brownian oscillator model [6]. These results closely match those of Eq. (2). The Brownian oscillator model does best at predicting spectroscopies relating to ground-state fluctuations, such as the PE, since it is derived by an expansion about the ground-state dynamics. Figure 2(b) displays $\ln S(t_1)$. $S(t_1)$ shows a pronounced nonexponential decay at long times, in contrast with the exponential decay predicted by the Bloch equations. The failure of the Bloch equations is due to the lack of time scale separation in $C(t)$.

Figure 3(a) shows the calculated 3PE signal. The $t_2=0$ section of the 3PE corresponds to the PE. The 3PE clearly shows the vibrational nature of the solvent dynamics during the t_2 period, in contrast with the PE. Pump-probe spectroscopy (PP) is closely related to the 3PE. We consider impulsive PP, where the pump and probe are ultrashort and the resulting emission is spectrally dis-

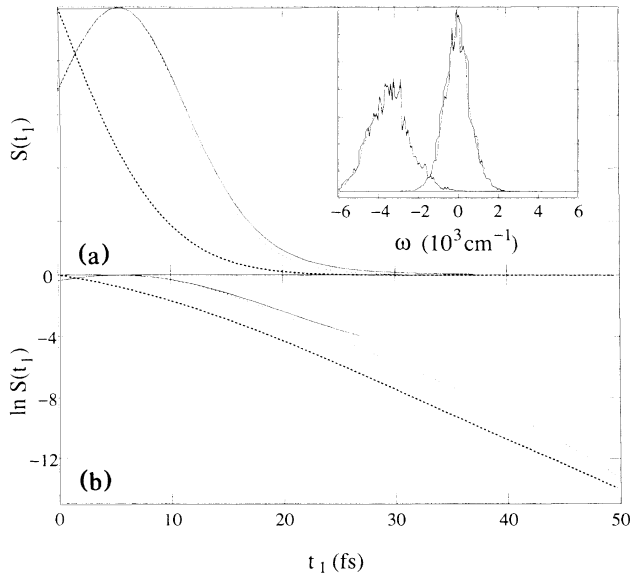

FIG. 2. (a) The two-pulse photon echo signal. Solid line, calculation of Eq. (2); dotted line, cumulant calculation; heavy dotted line, best fit of Bloch equations to the PE signal. (b) As in (a), but the logarithm of the signal is shown. Inset: Absorption and fluorescence.

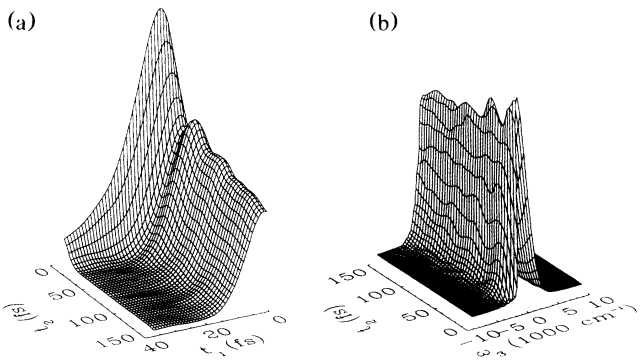

FIG. 3. (a) The three-pulse photon echo signal. (b) The impulsive pump-probe signal.

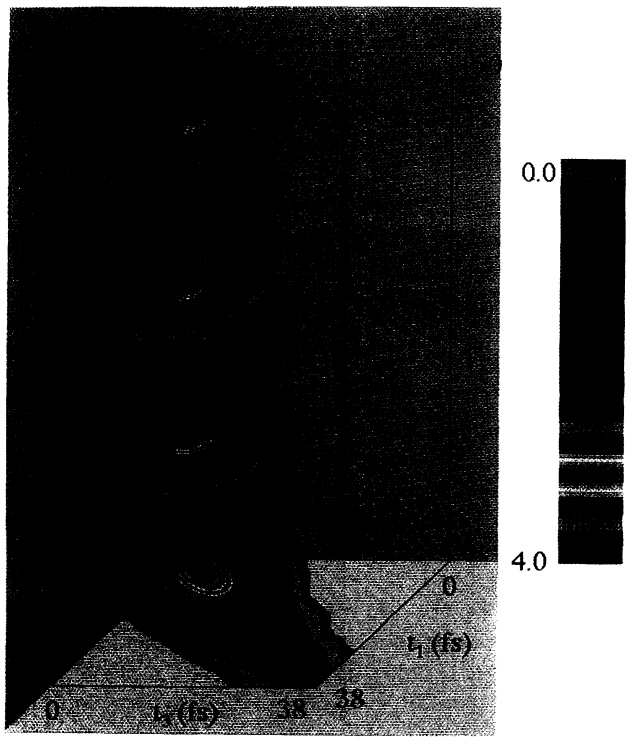

FIG. 4. The nonlinear polarization $|P^{(3)}(t_3,t_2,t_1)|^2$. The color map used is also shown. The values of $|P^{(3)}|^2$ were mapped into colors with the color map shown.

persed. The signal is

$$S_{PP}(\omega_3,t_2)=\mathrm{Re}\int_0^\infty e^{i\omega_3 t_3}P^{(3)}(t_3,t_2,t_1=0)dt_3.$$

Figure 3(b) shows S_{PP} for the present system. At $t_2=0$, S_{PP} is the same as the ordinary absorption line shape. As t_2 increases, the excited-state term shifts to the red, leading to a broadening and a growing asymmetry in the spectrum. The Stokes shift of the excited-state term is not predicted by the Bloch equations or by the stochastic model.

PP and PE are complementary special cases of the 3PE. The 3PE probes the full nonlinear polarization $P^{(3)}(t_1,t_2,t_3)$, whereas the PP depends only upon the $t_1=0$ plane of $P^{(3)}$, and the PE depends only on the $t_2=0$ plane. In physical terms, the PE probes the decay and rephasing of a coherence, whereas PP measures the dynamics of an excited-state population. The 3PE, however, contains both the coherence decay and rephasing and the population dynamics.

Nonlinear spectroscopies measure various aspects of $P^{(3)}(t_1,t_2,t_3)$. A complete measurement of $P^{(3)}$ as a function of its three time arguments could be done by using three ultrashort pulses followed by a fast detection of the signal. Figure 4 shows the complete $|P^{(3)}(t_3,t_2,t_1)|^2$. We first consider the $t_2=0$ plane. The PE signal is determined by $P^{(3)}$ in this plane. $P^{(3)}$ is seen to show an echo at times $t_3=t_1$, which means that rephasing of the initial coherence occurs. The $t_1=0$ plane of $P^{(3)}$ corresponds to the PP signal. As t_2 is increased $P^{(3)}$ decays faster with t_3. This corresponds to the broadening of the PP signal as the Stokes shift begins, since t_3 is the variable associated with the probe absorption line shape.

Finally, we consider $P^{(3)}$ for nonzero t_1 and t_2. As t_2 is increased from 0, relaxation processes prevent rephasing from occurring; $P^{(3)}$ is less peaked about $t_1=t_3$. Only at very short times can the thermal distribution of solvent environments be considered inhomogeneous; later spectral diffusion during t_2 destroys the echo. We also note that the vibrational dynamics of $C(t)$ is reflected in the oscillations of $P^{(3)}$.

In conclusion, the essential features of recent experiments in polar liquids, such as the non-Bloch decay of the PE signal and dynamics in the intermediate modulation regime, were captured in the present simulation. We were able to clarify the relation between various spectroscopic probes and the underlying molecular motion. In particular, we found that PP and 3PE experiments are more sensitive to vibrational dynamics than PE experiments. Finally, our analysis of $P^{(3)}(t_3,t_2,t_1)$ shows that spectral diffusion during the t_2 interval very rapidly destroys the echo character of the polarization.

The support of the National Science Foundation and the Air Force Office of Scientific Research is gratefully acknowledged. L.E.F. acknowledges the support of an NSF postdoctoral fellowship. N.B. thanks the NSF for an undergraduate research fellowship.

[1] J. Y. Bigot, M. T. Portella, R. W. Schoenlein, C. J. Bardeen, A. Migus, and C. V. Shank, Phys. Rev. Lett. **66**, 1138 (1991).
[2] E. T. J. Nibbering, D. A. Wiersma, and K. Duppen, Phys. Rev. Lett. **66**, 2464 (1991).
[3] R. G. DeVoe and R. G. Brewer, Phys. Rev. Lett. **50**, 1269 (1983).
[4] L. E. Fried and S. Mukamel, J. Chem. Phys. **93**, 3063 (1990).
[5] A. M. Walsh and R. F. Loring, J. Chem. Phys. **94**, 7575 (1991).
[6] S. Mukamel, Annu. Rev. Phys. Chem. **41**, 647 (1990); Y. J. Yan and S. Mukamel, J. Chem. Phys. **94**, 179 (1991).
[7] R. Kubo, Adv. Chem. Phys. **15**, 101 (1969).
[8] S. Mukamel, Phys. Rev. A **28**, 3480 (1983); R. F. Loring and S. Mukamel, Chem. Phys. Lett. **114**, 426 (1985).
[9] H. J. C. Berendsen, J. R. Grigera, and T. P. Straatsma, J. Chem. Phys. **91**, 6269 (1987).
[10] M. P. Allen and D. J. Tildesley, *Computer Simulations of Liquids* (Oxford Science Publications, Oxford, 1987).
[11] M. Maroncelli and G. R. Fleming, J. Chem. Phys. **89**, 5044 (1988).

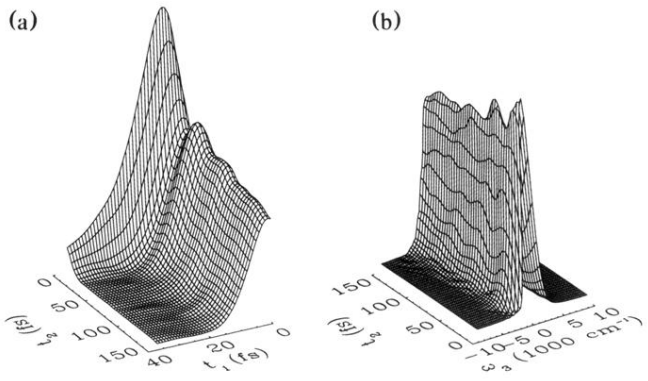

FIG. 3. (a) The three-pulse photon echo signal. (b) The impulsive pump-probe signal.

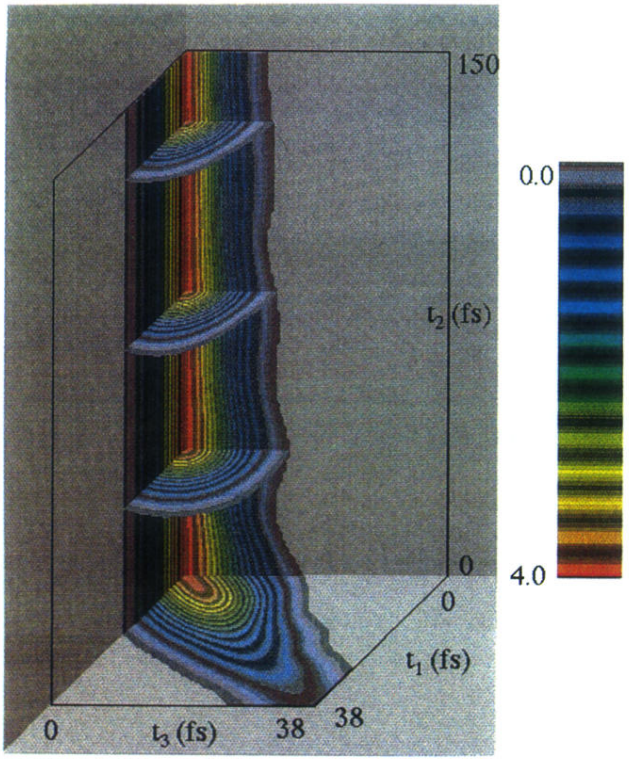

FIG. 4. The nonlinear polarization $|P^{(3)}(t_3,t_2,t_1)|^2$. The color map used is also shown. The values of $|P^{(3)}|^2$ were mapped into colors with the color map shown.